ELSEVIER

Process Biochemistry 36 (2000) 157–173

PROCESS BIOCHEMISTRY

www.elsevier.com/locate/procbio

Mass transfer and equilibrium studies for the sorption of chromium ions onto chitin

Yeşim Sağ *, Yücel Aktay

Department of Chemical Engineering, Faculty of Engineering, Hacettepe University, 06532 Beytepe, Ankara, Turkey

Received 21 February 2000; received in revised form 16 May 2000; accepted 27 May 2000

Abstract

The kinetics and equilibrium of chromium sorption onto chitin were studied with respect to pH, particle size, initial metal ion concentration, sorbent concentration and stirring rate. In order to select the main rate-limiting step in the overall uptake mechanism, a single external mass transfer diffusion model and intraparticular mass transfer diffusion models were used. External film mass transfer coefficients gave a mean value of 1.16×10^{-3} cm s^{-1}. Chromium sorption onto chitin was mainly located on the surface. However, the stirring rate had no noticeable effect on the overall uptake rate of chromium. This observation led to the conclusion that external mass transfer resistance was not the major limiting phenomenon. Intraparticle diffusion coefficients gave a mean value of 2.78×10^{-3} mmol g^{-1} $s^{-0.5}$ (0.17 mmol g^{-1} $h^{-0.5}$), indicating a poor intraparticular diffusion into the chitin or into the pores. The equilibrium isotherms were analysed using the monolayer and multilayer sorption models. Finally, the chromium binding capacity of chitin was compared with that of *Rhizopus arrhizus*, which possesses a high chitin content in the cell wall.

Keywords: Sorption; Chitin; *Rhizopus arrhizus*; External film mass transfer coefficient; Intraparticle diffusion coefficient; Sorption models

1. Introduction

Accumulation of heavy metals by micro-organisms or their products has been studied extensively. Most of the published reports on biosorption of metallic ions are aimed at assessing the metal-binding capacity, and only a few attempts have been made to elucidate the mechanism of binding. The biosorption mechanism depends strongly on the nature of the biosorbent. Algae, fungi and bacteria differ from each other in their composition, giving rise to different mechanisms of metal biosorption. To explore biosorption mechanisms, it is necessary to identify the functional groups involved in the biosorption process [1]. Chitin, a polymer of *N*-acetyl-D-glucosamine residues, is the second most common polymer produced by living beings. It is produced by fungi, insects, and a variety of marine animals and is able to chelate heavy metal ions. Therefore, studies on the interaction between heavy metal ions and chitin or *Rhizopus arrhizus* cells, a well-established biosorbent, are of interest in environmental biotechnology [2,3].

Chitin, a completely substituted polysaccharide carrying one amine or amide group per glucose ring (9% nitrogen), exhibits some metal uptake. Deacetylated chitin is called chitosan. The formation of a coordination complex between the metal and the chitin nitrogen or oxygen has been suggested. Ion exchange has also been suggested as a process that may be active in the uptake of certain metals by chitin or chitosan, however, the chitin/chitosan–metal biosorption mechanism has not been fully explained [2,4]. Sorption of chromium appears to occur by precipitation onto chitin with the formation of nodules of metal, a mechanism referred to the Eiden–Jewell effect [5]. In order to improve metal-binding abilities, some chemical modifications such as increasing the degree of deacetylation [6], crosslinking between the polymer chains [7] or grafting of functional groups [8] can be made. Chitin can be extracted in large quantities from crab and shrimp shells, saving the costs involved in landfilling the tons of crab and shrimp

* Corresponding author. Tel.: +90-312-2977444; fax: +90-312-2992124.

E-mail address: yesims@hacettepe.edu.tr (Y. Sağ).

0032-9592/00/$ - see front matter
PII: S0032-9592(00)00200-4

shells piling up along coastlines or from the broth of industrial fungal processes [9].

The precise mechanisms of metal ion binding have not been established for many of the biosorbents. In the present paper, it has been shown that intraparticle diffusion, external mass transfer and chemical binding reactions can be rate-controlling steps. The application of mass transfer diffusion models and equilibrium models would help in understanding the sorbent behaviour and aiding the scale-up of the process. Sorption kinetics of chromium onto chitin are mainly controlled by three consecutive steps including diffusion processes [10–13]:

1. chromium transport from the boundary film to the surface of the sorbent;
2. transfer of chromium from the surface to the intraparticular active sites;
3. uptake of the chromium ions on the active sites, via electrostatic and ionic interactions, sorption and intraparticular precipitation.

The last step is assumed to be rapid while steps 1 and 2 are the rate determining steps, either singly or in combination. Determination of the rate limiting steps in sorption is necessary in order to define the rate parameters for design purposes. In a well-agitated batch system, the boundary layer surrounding the particle is much reduced, reducing the external mass transfer coefficient; hence, intraparticular diffusion is more likely to be the rate controlling step [12,13].

1.1. External mass transfer diffusion model (or the boundary model)

The boundary model assumes that the surface concentration of chromium, C_s, is negligible at $t=0$, and consequently, intraparticle diffusion is negligible. The change in chromium concentration with respect to time is related to the liquid–solid mass transfer coefficient, β_L, by the equation [12–17]:

$$\frac{dC}{dt} = -\beta_L S(C - C_s) \quad (1)$$

where C is the liquid phase solid concentration at a time t, and $C=C_0$ at $t=0$; C_s the liquid phase solute concentration at the particle surface; and S the specific surface area for mass transfer.

After making the assumptions mentioned above, the previous equation can be simplified to

$$\left[\frac{d(C/C_0)}{dt}\right]_{t\to 0} = -\beta_L S \quad (2)$$

Since it was not possible to determine the specific surface area S, due to the poor porosity of chitin particles, the specific surface area is approximated as the external surface area. The particles are supposed to be spherical and S, calculated as the external surface compared with the solid/liquid ratio in the solution, gives

$$S = \frac{6m}{d_p \rho_{app}} \quad (3)$$

where m is the sorbent mass concentration in the solution, d_p the particle diameter and ρ_{app} the apparent volume mass of the sorbent.

1.2. Intraparticular mass transfer diffusion models

In the model developed by Weber and Morris [15] and McKay and Poots [16], the initial rate of intraparticular diffusion is calculated by linearisation of the curve $q=f(t^{0.5})$ [12,13]. Another kind of intraparticular diffusion model was proposed by Urano and Tachikawa (U&T) [18]. In this model the sorption rate is considered to be independent of the stirring speed and external diffusion to be negligible relative to the low overall sorption rate. The (U&T) model is given by the following equation [13,18]:

$$f\left(\frac{q}{q_m}\right) = -\left[\log\left(1-\left(\frac{q}{q_m}\right)^2\right)\right] = \frac{4\pi^2 D_i t}{2.3 d_p^2} \quad (4)$$

where q and q_m are the solute concentrations in the solid at t and $t\to\infty$, d_p the particle diameter and D_i the diffusion coefficient in the solid. Linearisation is carried out using the initial time of contact between 0 and 360 min.

1.3. Equilibrium sorption models

The most widely used isotherm equation for modelling of the biosorption equilibrium data is the Langmuir equation [19,20]

$$q_{eq} = \frac{aC_{eq}}{1+bC_{eq}} \quad (5)$$

where C_{eq} is the metal concentration in solution and $a=q_s b$. The Langmuir model assumes that each site accepts only one molecule, that sorbed molecules are organised as a monolayer, that all sites are energetically equivalent and that there is no interaction between sorbed molecules. The Langmuir equation obeys Henry's law at low concentrations.

The Freundlich expression is an empirical equation based on sorption on a heterogeneous surface. The Freundlich equation is commonly presented as [19,20]:

$$q_{eq} = a^0 C_{eq}^{b^0} \quad (6)$$

and the equation may be linearised by taking logarithms.

A further empirical isotherm has been developed by Redlich and Peterson (RP), incorporating three parameters [21]:

$$q_{eq} = \frac{K_R C_{eq}}{1+a_R C_{eq}^{\beta}} \quad (7)$$

where the exponent β, lies between 0 and 1. When $\beta = 1$, the Redlich–Peterson equation reduces to the Langmuir equation. When $\beta = 0$, Henry's law form results.

The theoretical model for multilayer sorption is [22,23]:

$$q_{eq} = \frac{Q_m B C_{eq}}{(C_s - C_{eq})[1 + (B-1)(C_{eq}/C_s)]} \quad (8)$$

where C_s is the saturation concentration of the solute, and B a constant relating to the energy of interaction with the surface. The linearised form of the BET equation is given as follows:

$$\frac{C_{eq}/C_s}{q_{eq}(1-(C_{eq}/C_s))} = \frac{1}{Q_m B} + \frac{(B-1)}{Q_m B}\frac{C_{eq}}{C_s} \quad (9)$$

The aim of this study was to understand the mechanisms that govern chromium removal by chitin, and to propose appropriate models for the kinetics and equilibrium of removal in a batch reactor. Batch studies were carried out to identify the rate controlling steps for chromium sorption by determining an external film mass transfer coefficient and an intraparticle diffusion coefficient. The equilibrium data were then analysed using Langmuir, Freundlich, Redlich–Peterson and BET sorption models and the characteristic sorption parameters for each isotherm were determined.

2. Materials and methods

2.1. Materials

Chitin prepared from crab shells poly(*N*-acetyl-1,4-β-D-glucopyranosamine)] $(C_8H_{13}NO_5)_n$ (Fluka 22720) was used for chromium removal. Before utilisation of the sorbent, the raw chitin was ground and sieved into three fractions as a function of particle diameter d_p (μm) — $250 < d_p < 420$, $420 < d_p < 595$ and $595 < d_p < 841$. Before and after sorption experiments, the chitin particles were weighed and no weight loss of the sorbent was observed at any pH examined. The degree of deacetylation (DD) of the chitin flakes was determined by a Fourier transform infrared (FTIR) spectroscope (Shimadzu 8100) using the following equation [6]:

$$\text{Degree of deacetylation } (\%) = \left[1 - \left(\frac{A_{1655}}{A_{3450}}\right)\frac{1}{1.33}\right]100 \quad (10)$$

where A_{1655} and A_{3450} are absorbency values at 1655 and 3450 cm^{-1} for carbonyl and hydroxyl peaks, respectively. Acetylation analysis gives a 27.2% DD.

R. arrhizus, a filamentous fungus, was obtained from the U.S. Department of Agriculture Culture Collection. *R. arrhizus* was grown aerobically in batch culture at 30°C and prepared for biosorption as described previously [24].

2.2. Preparation of sorption media

The stock solution of Cr(VI) (1.0 g l^{-1}) was prepared by dissolving a weighed quantity of potassium dichromate ($K_2Cr_2O_7$) in distilled water. The range of concentrations of prepared metal solutions varied between 0.481 and 4.808 mmol l^{-1}. Before mixing with the chitin flakes or fungal suspension, the pH of each was adjusted to the required value for the biosorption of Cr(VI) ions, by adding 1 mol l^{-1} of H_2SO_4.

2.3. Batch sorption experiments

Batch kinetics experiments were conducted at a constant temperature (25°C), in a rotary shaker, using 250-ml flasks. The sorption media consisted of a total volume of 100 ml. Before mixing the chitin flakes and the metal-bearing solution, 3-ml samples were taken from the sorption media. Subsequently, samples were taken at 5-min intervals at the beginning of sorption and at 15–30-min intervals before reaching equilibrium. Batch type contact studies were continued for 7 days. The sorption equilibrium was reached after 24 or 48 h, depending on the initial metal ion concentration and particle size. At higher initial metal ion concentrations or lower particle sizes, the variation of the unadsorbed Cr(VI) concentration in the solution was negligible after 420 min of contact time. After the equilibrium stage, long-term chromium sorption continued. In the U&T model, the sorbed Cr(VI) ion quantity per unit weight of chitin at the end of 7 days was q_m. In order to investigate the effects of stirring rate, sorption studies were performed in a batch-baffled and magnetically stirred reactor. The working volume of the reactor was 100 ml. The stirring rate was varied between 200 and 800 rpm. Fungal biosorption studies were carried out as described previously [24].

2.4. Analysis of Cr(VI) ions

The Cr(VI) content in the sorption medium was determined spectrophotometrically. The coloured complex of Cr(VI) ions with diphenyl carbazide was read at 540 nm [25].

3. Results and discussion

3.1. Investigation of sorption kinetics

In this study, chromium sorption kinetics onto chitin were investigated as a function of pH, particle size, initial metal ion concentration, sorbent concentration and stirring rate, using the three models of single diffusion previously described. Single independent models were chosen in order to estimate the relative influ-

ence of experimental parameters. Some of the models present multi-linearity, i.e. several portions of the curve were linear in a restricted range [26–28]. This could indicate that two or more phenomena were occurring successively. For the determination of intraparticle diffusion coefficients, which predominates in the range 10–60% of the adsorption region, correlations only take into account the first part of the curves. So, for the determination of the diffusion rates and related coefficients this first linear part is only considered to be an approximation of both intraparticular and external diffusion characteristics. Then a decreasing rate of sorption produces another curved portion leading to an equilibrium plateau.

3.1.1. Effect of pH

Chitin is a good sorbent for metal ions due to its high content of acetylamino and amino groups, which are responsible for chelating metal ions. The pH influences the metal chemistry in solution or the protonation or deprotonation of the polymer. Chromium forms stable complexes such as $Cr_2O_7^{2-}$, $HCrO_4^-$, CrO_4^{2-} and $HCr_2O_7^-$ and the fraction of any particular species is dependent upon chromium concentration and pH. A lower pH will cause the functional groups of chitin to be protonated to a higher extent and result in a stronger attraction for a negatively charged ion in the solution. Since the Cr(VI) ions in the solution are present in the form of dichromate ions which are negatively charged, they are attracted by the protonated amino groups of the chitin. For that reason, Cr(VI) ions are best adsorbed onto chitin at pH in the range 2.0–3.0. Beyond pH 6.0, the sorbent was also negatively charged and chromium removal was drastically reduced. This forms the base of the adsorption phenomenon, but overall metal removal process does not contain only this adsorption step, there is also transfer of the chromium ions from the bulk solution to the surface of the chitin particles which are in the form of flakes having a size distribution varying between 250 and 420, 420 and 595, and 595 and 841μm. Adsorption depends on the ionic interaction between those anionic metals and protonated active sites of the chitin. This might be expected to be a faster step compared with the external mass transfer of chromium onto the surface of chitin particles. Therefore, this external mass transfer must be the controlling step for the overall sorption process. The effect of pH on the external diffusion rates is given by a plot of C_t/C_0 versus time (Fig. 1a). The external film mass transfer coefficient, β_L, can be determined from the slope as $t \rightarrow 0$. According to the equation W&M, intraparticle diffusion is determined by a dependence on the square root of time, $t^{1/2}$, and is assessed from plots of q versus $t^{1/2}$. If intraparticle diffusion is a rate controlling step, then the plots should be linear; the slope of the linear section is determined and is defined as an intraparticle diffusion rate parameter, K. Fig. 1b shows a plot of q versus $t^{1/2}$ for the effect of pH on Cr(VI) sorption by chitin. According to the U&T equation, the slope of a plot of $f(q/q_m) = -\log(1-(q/q_m)^2)$ versus t gives the diffusion coefficient D_i' in the solid ($cm^2\ s^{-1}$) (Fig. 1c). As seen from Table 1, at lower pH values the attraction between the functional groups of chitin and anionic chromium ions gets stronger because of higher protonation extent of those acetylamino and amino groups. This effect causes the external mass transfer coefficient to increase. Considering the W&M intraparticle diffusion model, the internal diffusion coefficient also increases. These two phenomena can be assumed to take place combined in different proportions.

3.1.2. Effect of particle size

As seen from Fig. 2a–c and Table 2, particle size influences the sorption rate. As the particle size is decreased, the external surface of the chitin flakes increased. This decrease in the particle size decreased both the intraparticle diffusion resistance and the external mass transfer resistance. The initial external diffusion rate ($\beta_L S$) was increased by lowering the particle size of the sorbent. Under the same conditions, the intraparticle diffusion rate (k and initial slope of $f(q/q_m)$) increased. Increasing the particle size resulted in a greater time to reach equilibrium. The solute required more time to diffuse to the interior of the particle. The increased particle size will introduce a higher intraparticle diffusion resistance and will therefore have a lower internal diffusion coefficient. The existence on the same curve of various lines suggests that various intraparticle diffusion coefficients can be determined. This result can be attributed to diffusion in pores of different class sizes [17]. This distinction is also related to the size of the ion. Low sorption can be a result of poor diffusion as observed for 420–595 and 595–841 μm particle classes. In some cases, the linearisation of q versus $t^{1/2}$ gives a positive and significant ordinate intercept, indicating the influence of external rate control. Since the U&T model does not take external mass transfer resistance into account, it appears to be inadequate for the process.

3.1.3. Effect of initial metal ion concentration

As a rule, increasing the initial metal concentration results in a decrease in the initial rate of external diffusion (Fig. 3a), but an increase in the intraparticular diffusion rate according to the W&M model (Fig. 3b). Increasing the metal concentration in the solution reduced the diffusion of metal ions in the boundary layer and enchanges the diffusion in the chitin. These results are consistent with previous studies on copper and vanadium sorption onto chitosan [12,13]. In this study, it is interesting to observe that the external diffusion

rate decreased at initial metal ion concentrations lower than 1.968 mmol l^{-1}. At low initial metal ion concentrations, adsorption step occurred very fast owing to the large difference in concentration between the chitin surface and the boundary layer or a strong driving force. External transport can also become the rate-limiting step in systems, which have a dilute concentrate of sorbate. The U&T model is characterised by a poor fit to experimental results (Fig. 3c) and a meaningful change of intraparticular diffusion coefficients with initial concentrations was not observed. Table 3 confirms these conclusions. pH and metal concentration mainly influenced both metal and chitin chemistry in solution and so their effects were studied jointly. The chromium sorption onto chitin at pH 3.0 exhibited similar behaviour to diffusion mechanisms in chromium sorption at pH 2.0 (Table 4).

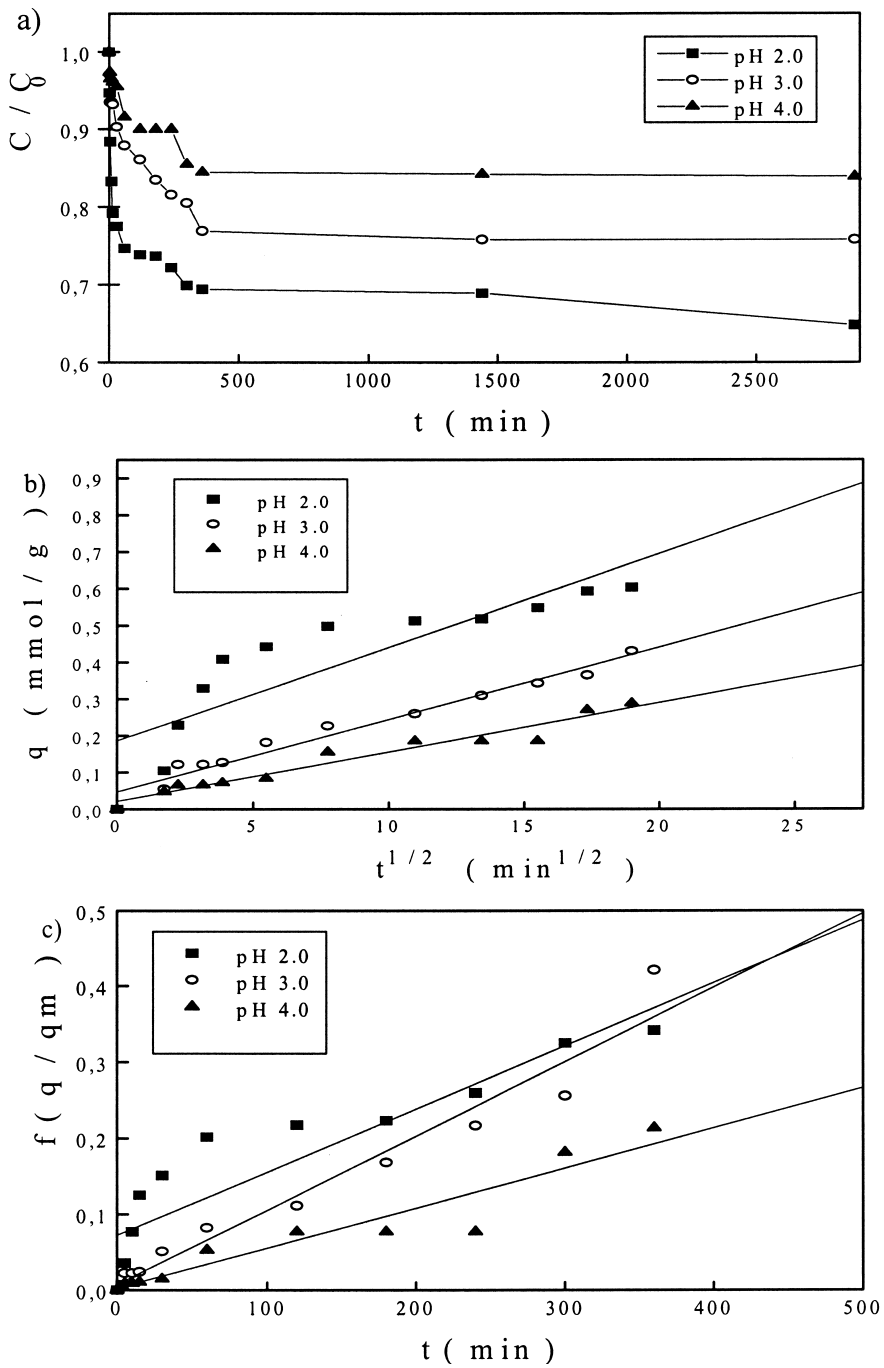

Fig. 1. Effect of pH on the sorption kinetics of Cr(VI) ions by chitin. (a) External mass transfer diffusion model; (b) intraparticular mass transfer diffusion model of Weber and Morris; (c) intraparticular mass transfer diffusion model of Urano and Tachikawa (C_0, 1.923 mmol l^{-1}; particle size, 250–420 μm; sorbent concentration, 1 g l^{-1}).

Table 1
Effect of pH on the external and intraparticular diffusion constants in Cr(VI) sorption by chitin[a]

pH	External diffusion		Internal diffusion		
	$\beta_L S$ ($\times 10^3$, s^{-1})	β_L ($\times 10^3$, cm s^{-1})	W&M model		U&T model
			K ($\times 10^3$, mmol g^{-1} $s^{-0.5}$)	$f(q/q_m)$ slope ($\times 10^5$, s^{-1})	D_i ($\times 10^{10}$, cm^2 s^{-1})
2.0	0.38	1.99	3.29	1.38	9.05
3.0	0.21	1.11	2.55	1.63	10.70
4.0	0.12	0.62	1.73	0.88	5.78

[a] C_0, 1.923 mmol l^{-1}; particle size, 250–420 μm; sorbent concentration, 1 g l^{-1}.

3.1.4. Effect of sorbent concentration

The variation in external film mass transfer coefficients and intraparticle diffusion coefficients calculated by both W&M and U&T models at different chitin concentrations is given in Table 5. As seen from Fig. 4a, an increase in chitin concentration generally increased the adsorbed Cr(VI) concentration because of an increasing adsorption surface area, whereas the adsorbed metal ion quantity q per unit weight of chitin decreased by increasing the chitin quantity (Fig. 4b and c). Chitin concentration (1 g l^{-1}) seems to be an optimum sorbent concentration with respect to both external and internal diffusion rates. Although the decrease in q with increase in sorbent concentration is due to complex interactions of several factors, there are two main reasons. First, the rate of sorption is reduced at high sorbent concentrations, and hence more time is needed to reach equilibrium. Second, the extent of desorption of sorbed ions from sorbent will increase with increase in sorbent concentration, as a result of collision of sorbent particles, and the potential of multilayer sorption will be reduced.

3.1.5. Effect of stirring rate

The effect of stirring speed (n) on the external and intraparticular diffusion is evaluated in terms of Reynolds number ($N_{Re} = nD_a^2\rho/\mu$) calculated from the diameter (D_a) and peripheral speed of the impeller (nD_a). Agitation influences the distribution of the solute in the bulk solution but can also act on the formation of the external boundary film. Increasing the Reynolds number from 2900 to 5800 increased the β_L value; this was not unexpected as increased turbulence reduces the film boundary layer surrounding the chitin particle (Table 6). At N_{Re} numbers lower than 5800, there was insufficient agitation to ensure the uniform distribution of sorbent and solute. Fig. 5a shows a good overlap of the curves at Reynolds number in the range 5800–11 600. Increasing the Reynolds number beyond 5800, however, did not raise the β_L value, indicating that external film mass transfer was not the rate-limiting step in a well-agitated vessel. At N_{Re} numbers higher than 11 600, the strong shear forces may have interfered with sorption, damaging the chitin particles. Since the initial external diffusion rate decreased with increasing particle size, the stirrer speed becomes important in overcoming external mass transfer resistances in a particle size range 595–841 μm. In this particle size range, the highest initial external diffusion rate was obtained at $N_{Re} = 8700$ (Table 7). Comparison of intraparticle diffusion coefficients determined for different stirrer speeds and particle size ranges, 250–420 and 595–841 μm showed that variation of agitation had little effect on the internal diffusion rate (K) value (Fig. 5b). This was not unexpected as agitation only influences the external transport step. However, the U&T model seemed to be affected significantly by a variation of the agitation speed, contrary to previous hypotheses. This confirms the inadequacy of this model for the sorption of Cr(VI) by chitin (Fig. 5c). This model was established with hypotheses such as a negligible influence of external diffusion in the sorption kinetic control. The slight effect of agitation implies that external mass transfer is not the sole rate-limiting phase, and confirms that intraparticle diffusion resistance needs to be included in the analysis of overall sorption. These deviations from the models also indicate that single models are not sufficient to describe experimental points accurately.

In this study, the external film mass transfer coefficient, β_L, was 1.99×10^{-3} cm s^{-1} with an external diffusion rate of 0.38 s^{-1} at optimum values of all the parameters examined (at pH 2.0, 250–420 μm particle size range, 1.968 mmol l^{-1} initial metal ion concentration and 1.0 g l^{-1} sorbent concentration). The external film mass transfer coefficients had a mean value of 1.16×10^{-3} cm s^{-1}. The same order of magnitude for external diffusion rate was observed for uranium sorption by glutamate glucan (around 0.4×10^{-3} s^{-1}). With vanadium this rate approximates a mean value of 2×10^{-3} s^{-1} ($\beta_L = 17 \times 10^{-3}$ cm s^{-1}) [13]. For copper and mercury sorption onto chitosan, McKay et al. [17] calculated a β_L coefficient equal to 8.5×10^{-3} and 4×10^{-3} cm s^{-1}, respectively. For uranium sorption by modified chitosans, this value approximates a mean value of 5.8×10^{-3} cm s^{-1} [29,30]. Findon et al. [12] report external diffusion coefficients changing between

63.6×10^{-3} and 5.4×10^{-3} cm s^{-1} with experimental parameters for copper sorption by chitosan.

For intraparticular diffusion rates, the model defined by the Weber and Morris gave the best fit to experimental results. The intraparticle diffusion coefficient, K, was determined as 3.29×10^{-3} mmol g^{-1} $s^{-0.5}$ (0.20 mmol g^{-1} $h^{-0.5}$) at optimum values of all the parameters examined. Intraparticle diffusion coefficients had a mean value of 2.78×10^{-3} mmol g^{-1} $s^{-0.5}$ (0.17 mmol g^{-1} $h^{-0.5}$). In the literature, the W&M model is generally applied and gives a mean value for vanadium between 1.18 and 9 mmol g^{-1} $h^{-0.5}$ [13]. For uranium sorption by modified chitosan, these values are set between 0.13 and 1.3 mmol g^{-1} $h^{-0.5}$ [29,30]. Chromium sorption by chitin appeared to be less controlled by diffusion mechanisms than vanadium and uranium uptake by chitosan. Yang and Zall [31] compared sorption performances and kinetic characteristics

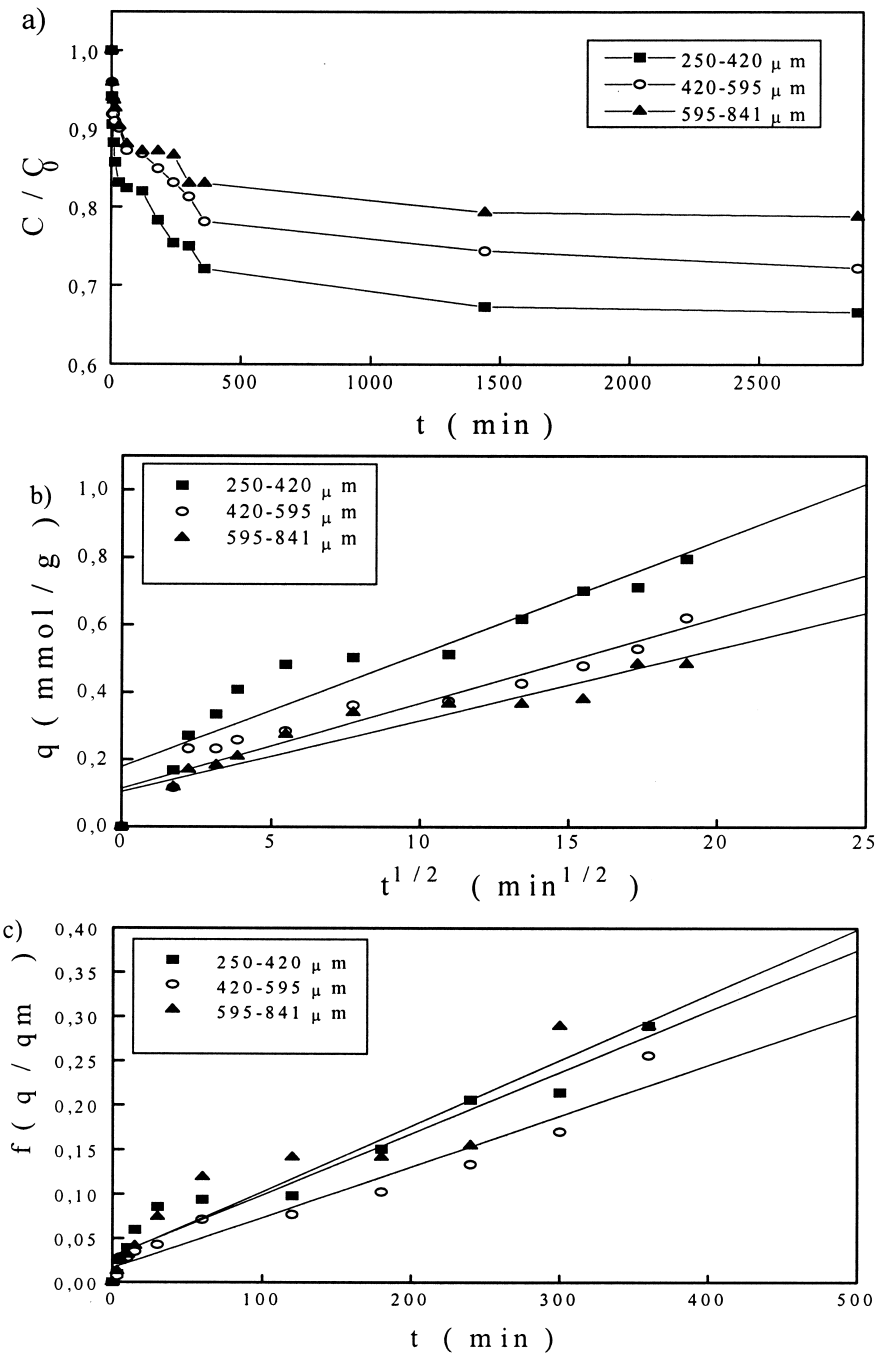

Fig. 2. Effect of particle size on the sorption kinetics of Cr(VI) ions by chitin. (a) External mass transfer diffusion model; (b) intraparticular mass transfer diffusion model of Weber and Morris; (c) intraparticular mass transfer diffusion model of Urano and Tachikawa (pH 2.0; C_0, 2.885 mmol l^{-1}; sorbent concentration, 1 g l^{-1}).

Table 2
Effect of particle size on the external and intraparticular diffusion constants in Cr(VI) sorption by chitin[a]

Particle size (μm)	External diffusion		Intraparticular diffusion		
	$\beta_L S$ ($\times 10^3$, s^{-1})	β_L ($\times 10^3$, cm s^{-1})	W&M model		U&T model
			K ($\times 10^3$, mmol g^{-1} $s^{-0.5}$)	$f(q/q_m)$ slope ($\times 10^5$, s^{-1})	D_i ($\times 10^{10}$, cm^2 s^{-1})
250–420	0.32	1.67	4.33	1.15	7.53
420–595	0.27	2.14	3.27	0.95	14.30
595–841	0.20	2.27	2.74	1.23	37.10

[a] pH 2.0; C_0, 2.885 mmol l^{-1}; sorbent concentration, 1 g l^{-1}.

(by a diffusion equation similar to the model of Weber and Morris) of copper, zinc, cadmium, chromium and lead onto chitosan and intraparticular diffusion rates were found to be 2.31, 0.94, 1.25, 0.83 and 0.28 mmol g^{-1} $h^{-0.5}$, respectively. Findon et al. [12] obtained an average value of 0.52 mmol g^{-1} $h^{-0.5}$ for the intraparticular diffusion coefficient of Cu(II) ions in chitosan. Diffusion coefficients were significantly lower than those obtained in water or porous solids, indicating a poor intraparticular diffusion into the solid or into the pores [32].

3.2. Investigation of equilibrium parameters

3.2.1. Effect of pH

To determine the equilibrium isotherms, initial Cr(VI) ion concentrations were varied between 0.481 and 4.808 mmol l^{-1} while the chitin concentration in each sorption medium was kept constant at 1.0 g l^{-1}. The sorption relationship was studied by examining the closeness of fit of various sorption isotherm models. The sorption constants calculated according to the Langmuir, Redlich–Peterson, BET and the Freundlich sorption models at different pH values are listed in Table 8. The Langmuir equation was linearised by plotting $1/q_{eq}$ versus $1/C_{eq}$ to determine the Langmuir constants from the slope $1/a$ and the intercept b/a. The amount of adsorbate per unit weight of adsorbent to form a complete monolayer on the surface is q_s and b is the ratio of adsorption/desorption rates and a large value of b implies strong bonding. The three parameters, a_R, K_R and β, given by the Redlich–Peterson sorption model were estimated from the equilibrium sorption data of Cr(VI) ions using an MS Excel 7.0 computer program. Since the poor diffusion in the solid, or the limitation of diffusion to a thin layer, implies that good overall sorption is possibly due to multilayer sorption, the BET model describing multilayer sorption was also applied to sorption equilibrium data of Cr(VI) ions onto chitin. The BET equation was linearised by plotting $(C_{eq}/C_s)/q_{eq}(1 - C_{eq}/C_s)$ versus C_{eq}/C_s to determine the BET constants from the slope $(B-1)/Q_mB$ and the intercept $1/Q_mB$ (Fig. 6). Finally, the intercept of the linearised Freundlich equation, a^0, is an indication of the sorption capacity of the sorbent; the slope, b^0, indicates the effect of concentration on the sorption capacity and represents the sorption intensity (Fig. 7). The values of the sorption constants obtained from the sorption isotherms confirm pH optima determined from the external and intraparticle diffusion rates for the uptake of Cr(VI) ions. Since increasing the pH diminishes electrostatic repulsion, the optimum pH for Cr(VI) sorption by chitin is reached at pH around 2. In addition, at high pH conditions the percentage of dichromate also decreases and, consequently, the chromium sorption was reduced. The correlation coefficients (R) were generally very high for the various models. However, the Freundlich model provided the best fit with experimental and predicted values at all pH values, even though this equation was derived for monolayer sorption. The Freundlich isotherm is an empirical model assuming a logarithmic decrease in the heat of sorption with the fraction of surface covered by the sorbed solute. Biological surfaces are expected to have heterogeneous energies for sorbing metals, and therefore a good fit was expected. The BET equation was not satisfactory to correlate the experimental isotherms. This is not surprising since the BET isotherm does not consider the heterogeneity of the sorbent surface and the lateral interactions between the sorbed molecules.

In this study, crab shell chitin with a 27.2% deacetylation degree (DD) was used. The number of Cr(VI) ions sorbed onto chitin is reported to increase with the increase of the DD. Kim et al. [6] report that the q_s values for the deacetylated crab shell chitins with 46.8, 36.3, and 10.7% DDs at pH 3.0 are 2.054, 1.350, and 0.349 mmol g^{-1}, respectively, which are again proportional to the increase of the DD of the chitin. This is mainly due to the increase of $-NH_3^+$ groups in chitin with a high DD and the low pH of the system. However, a high DD of chitosan brings an instability in acidic solutions owing to the increased solubility. Metal-containing industrial waste waters are strongly acidic and this restricts the use of chitosan as a metal scavenger, especially in the case of chromium.

3.2.2. Effect of particle size

The equilibrium uptake was influenced by the size distribution of sorbent particles (Fig. 8). Maximum uptake was a function of the specific area or external surface of the sorbent. Thus, smaller the particle, larger is the surface area. It is clear that the Langmuir constant, q_s, the BET constant, Q_m, and the Freundlich constant, a^0, decreased with increase in mean chitin diameter, suggesting that the smaller particles tend to have a higher capacity for Cr(VI) (Table 9). If sorption capacity is independent of the particle size, it would indicate that all the sorbent mass was saturated; the solute is able to diffuse even at the centre of the particle. On the other hand, a large size of Cr(VI) ions could explain a restriction in the diffusion of solute. A comparison of sorption capacities using the external surface would give a poor correlation — maximum uptake at equilibrium is not directly proportional to the

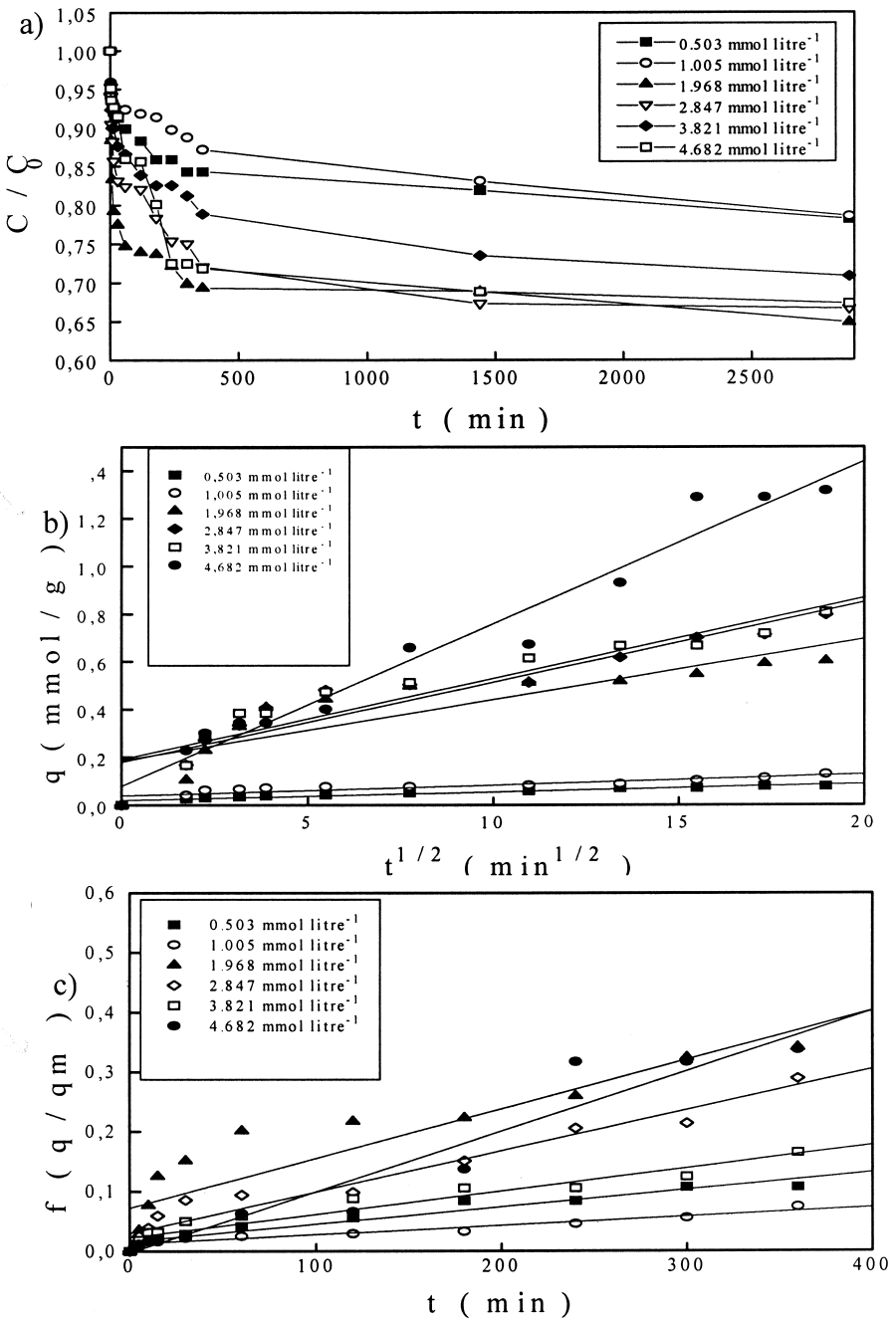

Fig. 3. Effect of initial metal ion concentration on the sorption kinetics of Cr(VI) ions by chitin. (a) External mass transfer diffusion model; (b) intraparticular mass transfer diffusion model of Weber and Morris; (c) intraparticular mass transfer diffusion model of Urano and Tachikawa (pH 2.0; particle size, 250–420 μm; sorbent concentration, 1 g l^{-1}).

Table 3
Effect of initial metal ion concentration on the external and intraparticular diffusion constants in Cr(VI) sorption by chitin at pH 2.0[a]

C_i (mmol l^{-1})	External diffusion		Intraparticular diffusion		
	$\beta_L S$ ($\times 10^3$, s^{-1})	β_L ($\times 10^3$, cm s^{-1})	W&M model	U&T model	
			K ($\times 10^3$, mmol g^{-1} $s^{-0.5}$)	$f(q/q_m)$ slope ($\times 10^5$, s^{-1})	D_i ($\times 10^{10}$, cm^2 s^{-1})
0.503	0.22	1.13	0.45	0.37	2.40
1.005	0.21	1.09	0.58	0.25	1.64
1.968	0.38	1.99	3.29	1.38	9.05
2.847	0.32	1.67	4.33	1.15	7.53
3.821	0.26	1.34	4.37	0.65	4.25
4.682	0.22	1.14	8.78	1.70	11.1

[a] Particle size, 250–420 μm; sorbent concentration, 1 g l^{-1}.

Table 4
Effect of initial metal ion concentration on the external and intraparticular diffusion constants in Cr(VI) sorption by chitin at pH 3.0[a]

C_i (mmol l^{-1})	External diffusion		Intraparticular diffusion		
	$\beta_L S$ ($\times 10^3$, s^{-1})	β_L ($\times 10^3$, cm s^{-1})	W&M model	U&T model	
			K ($\times 10^3$, mmol g^{-1} $s^{-0.5}$)	$f(q/q_m)$ slope ($\times 10^5$, s^{-1})	D_i ($\times 10^{10}$, cm^2 s^{-1})
0.521	0.17	0.87	0.32	0.33	2.18
1.036	0.19	1.01	0.67	0.57	3.71
1.868	0.21	1.11	2.55	1.63	10.7
2.927	0.24	1.28	3.02	0.60	3.93
3.795	0.21	1.12	3.43	0.47	3.05
4.718	0.18	0.94	6.48	1.15	7.53

[a] Particle size, 250–420 μm; sorbent concentration, 1 g l^{-1}.

Table 5
Effect of sorbent concentration on the external and intraparticular diffusion constants in Cr(VI) sorption by chitin[a]

Sorbent concentration (g l^{-1})	External diffusion		Intraparticular diffusion		
	$\beta_L S$ ($\times 10^3$, s^{-1})	β_L ($\times 10^3$, cm s^{-1})	W&M model	U&T model	
			K ($\times 10^3$, mmol g^{-1} $s^{-0.5}$)	$f(q/q_m)$ slope ($\times 10^5$, s^{-1})	D_i ($\times 10^{10}$, cm^2 s^{-1})
0.50	0.25	2.57	3.91	1.08	7.09
0.75	0.31	2.19	2.77	0.70	4.58
1.00	0.38	1.99	3.29	1.38	9.05
1.50	0.27	0.94	0.92	0.23	1.53
2.00	0.17	0.43	1.21	0.40	2.62
2.50	0.13	0.27	0.74	0.23	1.53

[a] pH 2.0; C_0, 1.923 mmol l^{-1}; particle size, 250–420 μm.

specific surface area. For example, the ratio between 250 and 420, and 595 and 841 μm particle sizes in external surface was almost 2.14, but the resulting sorption capacity only decreased by 17%. This would suggest that the control of the equilibrium concentration was not conditioned by the external surface alone. Chitin shows a concentration profile, which indicated a low diffusion in the centre of the particles and, for particles of greater diameters, sorption occurred into a thin layer. Consequently, uptake capacity is a function of both residual metal ion concentration in solution and the particle size of the polymer.

3.3. Comparison of the sorption of chromium onto chitin with *R. arrhizus*

R. arrhizus is known for its strong metal-sorbent properties. *Rhizopus* species have both chitin and chitosan as cell-wall components responsible for heavy metal uptake and their productivity of chitin/chitosan can be as high as 58% of the cell-wall mass [33]. In order to compare sorption capacities of all cells of *R. arrhizus* and chitin, the experimental data for all cells of *R. arrhizus* were modelled with the Langmuir and Freundlich isotherm equations (Fig. 9) and the constants

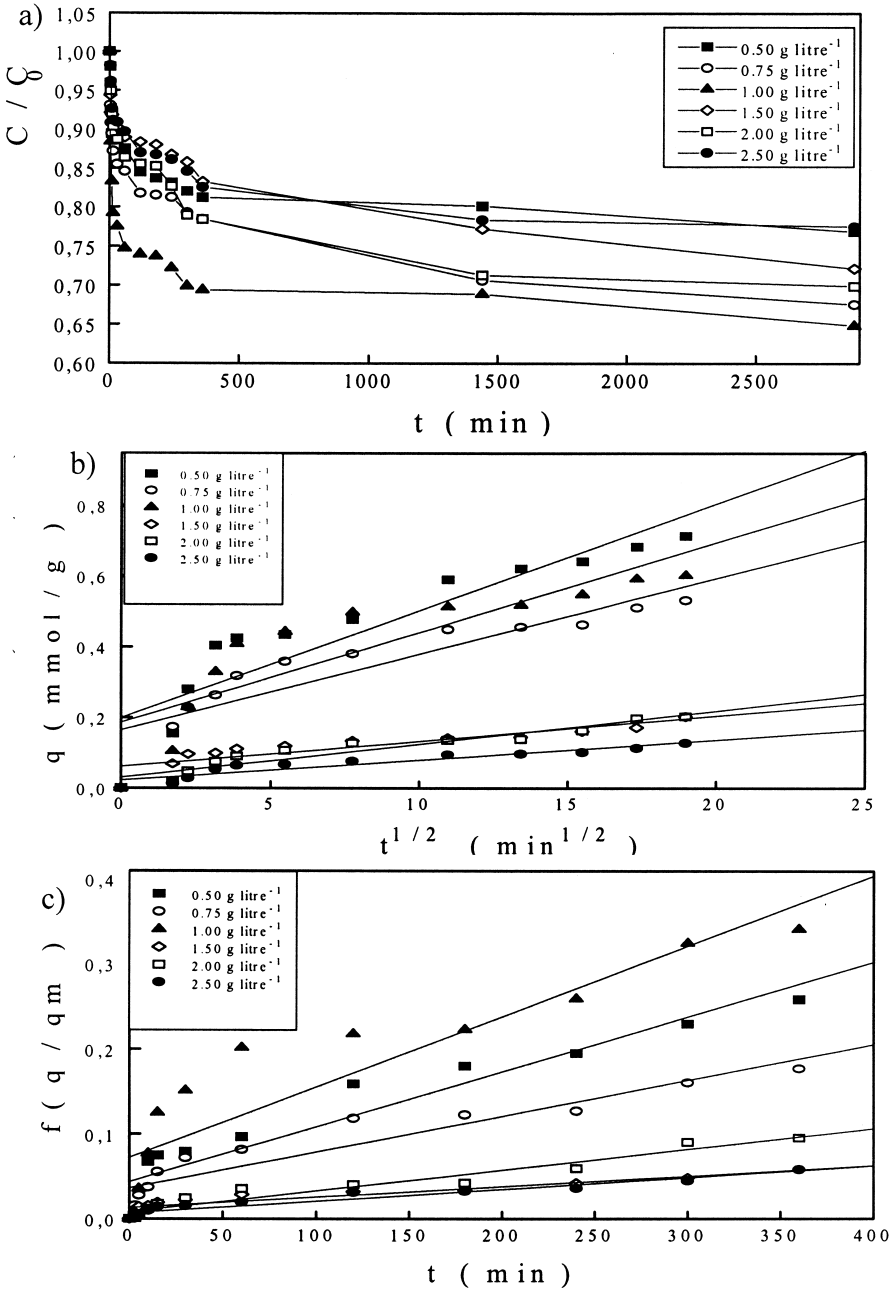

Fig. 4. Effect of sorbent concentration on the sorption kinetics of Cr(VI) ions by chitin. (a) External mass transfer diffusion model; (b) intraparticular mass transfer diffusion model of Weber and Morris; (c) intraparticular mass transfer diffusion model of Urano and Tachikawa (pH 2.0; C_0, 1.923 mmol l^{-1}; particle size, 250–420 μm).

Table 6
Effect of stirring rate on the external and intraparticular diffusion constants in Cr(VI) sorption by chitin in a particle size range 250–420 μm[a]

N_{Re}	External diffusion		Intraparticular diffusion		
	$\beta_L S$ ($\times 10^3$, s^{-1})	β_L ($\times 10^3$, cm s^{-1})	W&M model	U&T model	
			K ($\times 10^3$, mmol g^{-1} $s^{-0.5}$)	$f(q/q_m)$ slope ($\times 10^5$, s^{-1})	D_i ($\times 10^{10}$, cm^2 s^{-1})
2900	0.11	0.56	1.90	3.57	23.3
5800	0.14	0.73	3.37	5.68	37.2
8700	0.12	0.62	3.16	5.03	32.9
11 600	0.11	0.59	2.86	4.92	32.2

[a] pH 2.0; C_0, 1.923 mmol l^{-1}; sorbent concentration, 1.0 g l^{-1}.

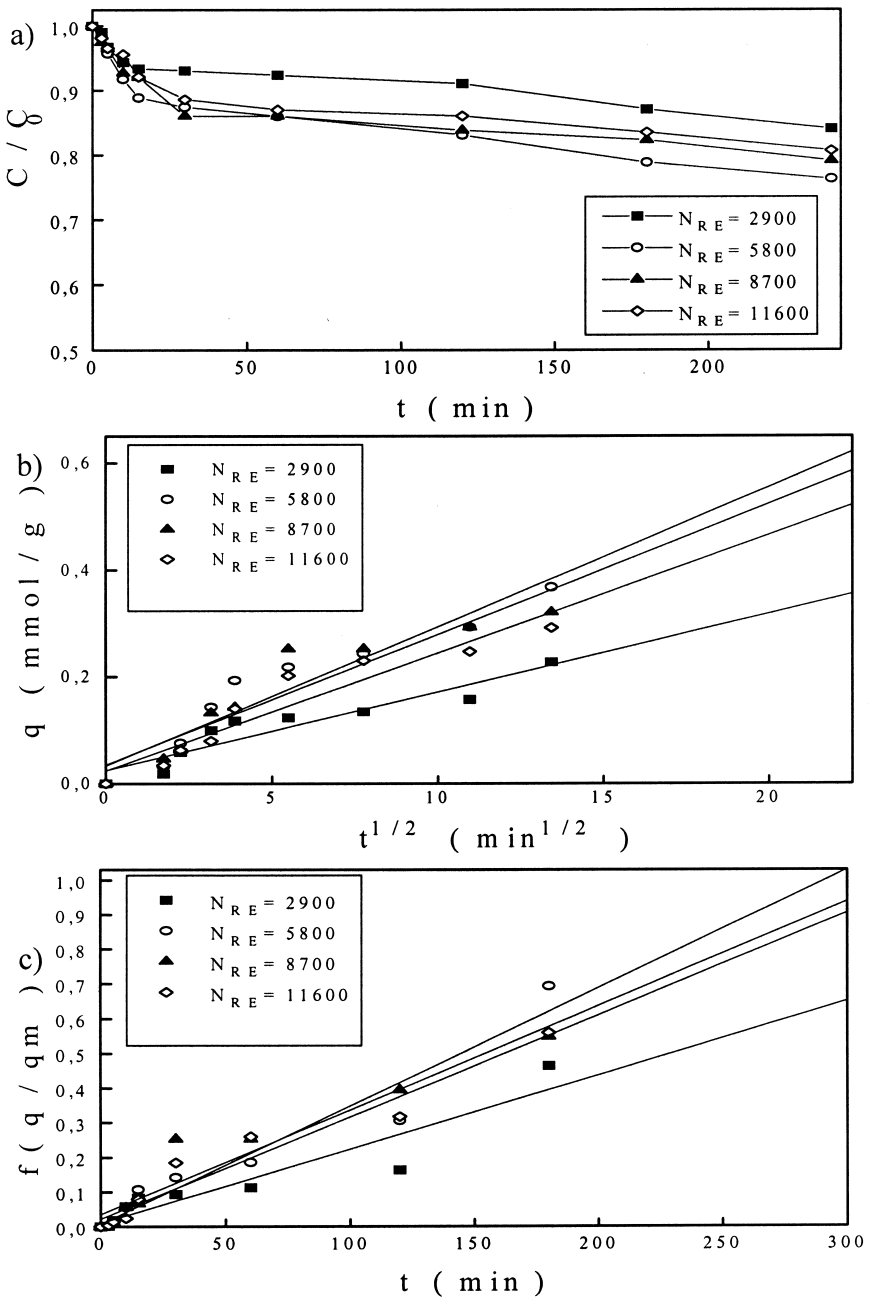

Fig. 5. Effect of stirring rate on the sorption kinetics of Cr(VI) ions by chitin. (a) External mass transfer diffusion model; (b) intraparticular mass transfer diffusion model of Weber and Morris; (c) intraparticular mass transfer diffusion model of Urano and Tachikawa (pH 2.0; particle size, 250–420 μm; C_0, 1.923 mmol l^{-1}; sorbent concentration, 1.0 g l^{-1}).

Table 7
Effect of stirring rate on the external and intraparticular diffusion constants in Cr(VI) sorption by chitin in a particle size range 595–841 μm[a]

N_{Re}	External diffusion		Intraparticular diffusion		
	$\beta_L S$ ($\times 10^3$, s^{-1})	β_L ($\times 10^3$, cm s^{-1})	W&M model	U&T model	
			K ($\times 10^3$, mmol g^{-1} $s^{-0.5}$)	$f(q/q_m)$ slope ($\times 10^5$, s^{-1})	D_i ($\times 10^{10}$, cm^2 s^{-1})
2900	0.07	0.74	2.28	6.05	182
5800	0.08	0.91	3.20	7.95	239
8700	0.11	1.24	2.95	6.17	185
11 600	0.10	1.08	2.66	5.02	151

[a] pH 2.0; C_0, 1.923 mmol l^{-1}; sorbent concentration, 1.0 g l^{-1}.

Table 8
Effect of pH on the sorption isotherm coefficients of the Langmuir, Redlich–Peterson, BET and Freundlich models[a]

pH	Langmuir model				Redlich–Peterson model				BET model			Freundlich model		
	q_s (mmol g^{-1})	b (l $mmol^{-1}$)	a (l g^{-1})	R	K_R (l g^{-1})	a_R ($mmol^{\beta+1}$ g^{-1} $l^{-\beta}$)	β	R	Q_m (mmol g^{-1})	B	R	a^0 ($mmol^{b^0+1}$ g^{-1} l^{-b^0})	b^0	R
2.0	1.946	0.335	0.652	0.980	0.703	0.645	0.229	0.993	0.393	12.809	0.944	0.464	0.835	0.992
3.0	1.808	0.221	0.400	0.988	0.542	0.649	0.453	0.972	0.253	19.793	0.975	0.312	0.875	0.989
4.0	1.573	0.194	0.305	0.986	0.265	0.105	0.546	0.985	0.239	9.330	0.964	0.243	0.920	0.986

[a] Particle size, 250–420 μm; sorbent concentration, 1 g l^{-1}.

Table 9
Effect of particle size on the sorption isotherm coefficients of the Langmuir, Redlich–Peterson, BET and Freundlich models[a]

Particle size (μm)	Langmuir model				Redlich–Peterson model				BET model			Freundlich model		
	q_s (mmol g^{-1})	b (l $mmol^{-1}$)	a (l g^{-1})	R	K_R (l g^{-1})	a_R ($mmol^{\beta+1}$ g^{-1} $l^{-\beta}$)	β	R	Q_m (mmol g^{-1})	B	R	a^0 ($mmol^{b^0+1}$ g^{-1} l^{-b^0})	b^0	R
250–420	1.946	0.335	0.652	0.980	0.703	0.645	0.229	0.993	0.393	12.809	0.944	0.464	0.835	0.992
420–595	1.816	0.252	0.457	0.987	0.682	1.008	0.256	0.983	0.309	12.412	0.947	0.347	0.866	0.985
595–841	1.616	0.235	0.380	0.994	0.530	0.845	0.255	0.979	0.260	15.222	0.988	0.292	0.847	0.990

[a] pH 2.0; sorbent concentration, 1 g l^{-1}.

derived are listed in Table 10. All cells of *R. arrhizus* and chitin reached equilibrium uptake values of 0.850 mmol Cr(VI) (g dry cell)$^{-1}$ and 0.577 mmol Cr(VI) g^{-1}, respectively, in a sorption medium containing 1.923 mmol Cr(VI) l^{-1}. The chromium sorption yields on all cells that can be mainly attributed to sorption to the cell walls and chitin were estimated to be 67 and 38%, respectively. Although chitin/chitosan only constitutes 17% of the cells [9], it seems to be responsible for 60% of the total Cr(VI) removal.

4. Conclusions

Chromium sorption onto chitin is influenced by parameters such as pH, particle size and initial metal ion concentration. This effect is noticeable on both kinetic and equilibrium aspects. A good correlation of experimental results with the linearised form of the external and internal mass transfer diffusion models indicates that diffusion mechanisms control sorption kinetics. Correlation coefficients vary between 0.865 and 0.995. The existence on the same curve of various lines suggests that two or more transport phenomena occur successively. However, a real approach of global diffusion would require a combined model, which is much more complicated to solve.

Sorption is a fast step compared with the external mass transfer of chromium onto the surface of chitin particles. Therefore, this external mass transfer must be the controlling step for the overall sorption process. There might also be an internal diffusion of chromium ions into a thin layer of the chitin particles. Although chitin particles are not considered to be porous, they

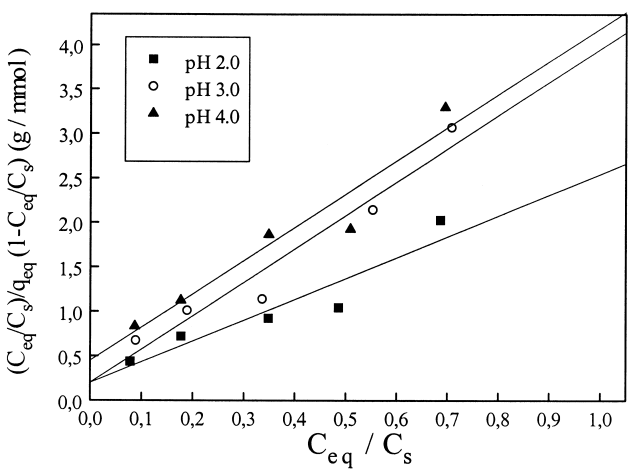

Fig. 6. The BET sorption isotherms obtained at different pH values for Cr(VI) sorption onto chitin (particle size, 250–420 μm; sorbent concentration, 1 g l^{-1}).

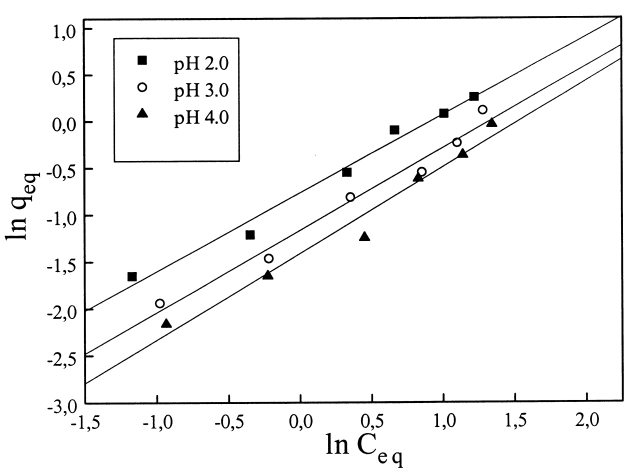

Fig. 7. The Freundlich sorption isotherms obtained at different pH values for Cr(VI) sorption onto chitin (particle size, 250–420 μm; sorbent concentration, 1 g l^{-1}).

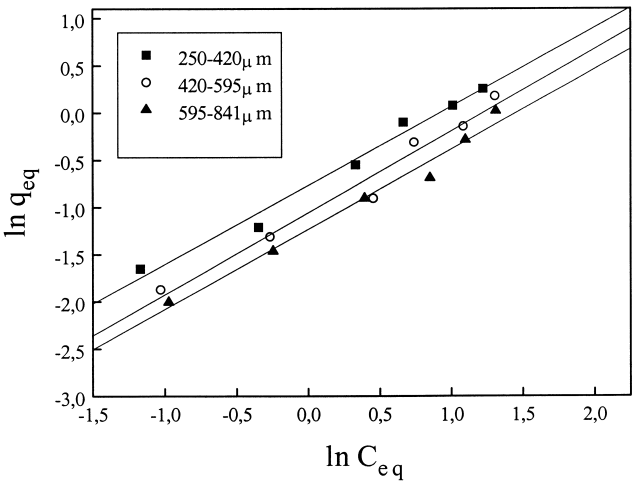

Fig. 8. The Freundlich sorption isotherms obtained at different particle sizes for Cr(VI) sorption onto chitin (pH 2.0; sorbent concentration, 1 g l^{-1}).

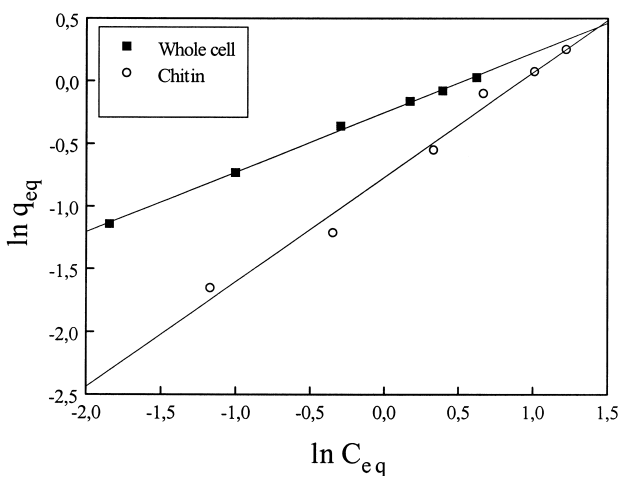

Fig. 9. Comparison of the Freundlich sorption isotherms for Cr(VI) sorption by *R. arrhizus* and chitin (pH 2.0; sorbent concentration, 1 g l^{-1}).

Table 10
Comparison of the sorption isotherm coefficients for Cr(VI) sorption by *R. arrhizus* and chitin[a1]

	Langmuir constants			Freundlich constants	
	q_s (mmol g^{-1})	b (l $mmol^{-1}$)	a (l g^{-1})	a^0 ($mmol^{b^0+1}$ g^{-1} l^{-b^0})	b^0
Whole cell	1.135	2.392	2.714	0.777	0.476
Chitin	1.946	0.335	0.652	0.464	0.835

[a] pH 2.0; sorbent concentration, 1 g l^{-1}.

will contain some micropores as well as roughness on their surfaces. Considering the size of chromium ions, the penetration of those anions into these small pores could be ruled out. Thus, it can be assumed that the sorption of chromium ions only occurs on the external surface of the chitin flakes and the total uptake capacity and the rate of sorption depend on this surface area. In this case, the sorption rate would be greatly influenced by the stirring rate. The liquid phase external mass transfer resistance around the chitin flakes can be reduced by vigorous agitation. However, the results show that the sorption rate does not seem to be much sensitive to stirring rate. Therefore, assuming there is solely external mass transfer without an internal diffusion step is not justified. As the particle size is decreased, the external surface area of the chitin flakes will be increased. This decrease in the particle size decreases both the intraparticle diffusion resistance and the external mass transfer resistance. As confirmed by the experimental results, the enhancement in total metal uptake and sorption rate owing to the smaller particles used is attributed to these reduced resistances as mentioned above. For the sorption of chromium ions, this enhancement is most likely to be interpreted as the reduced external mass transfer resistance surrounding the chitin flakes. However, the control of the initial, equilibrium and final concentration is not conditioned only by the external surface. For particles of greater diameters, only part of the chitin particle is saturated, and both kinetics and equilibrium are affected. Intraparticular diffusion is reduced and only the external surface, or a thin layer of the sorbent, is able to sorb chromium. The inadequacy of the single intraparticular diffusion model also implies that a combined effect of the two mechanisms is probable. The model defined by Urano and Tachikawa gives a poor fit to experimental results, defined with the hypothesis that external diffusion has not to be taken into account for the kinetic profile.

Acknowledgements

The authors wish to thank TÜBİTAK, the Scientific and Technical Research Council of Turkey, for the partial financial support of this study (Project No YDABÇAG, 199Y095).

References

[1] Ashkenazy R, Gottlieb L, Yannai S. Characterization of acetone-washed yeast biomass functional groups involved in lead biosorption. Biotechnol Bioeng 1997;55:1–10.
[2] Volesky B. Biosorption by fungal biomass. In: Volesky B, editor. Biosorption of Heavy Metals. Boca Raton, FL: CRC Press, 1990.
[3] Ngah WSW, Isa IM. Comparison study of copper ion adsorption on chitosan, Dowex A-1, and Zerolit 225. J Appl Polym Sci 1998;67:1067–70.
[4] McKay G, Ho YS, Ng JCY. Biosorption of copper from waste waters: a review. Sep Purif Methods 1999;28:87–125.
[5] Eiden CA, Jewell CA, Wightman JP. Interaction of lead and chromium with chitin and chitosan. J Appl Polym Sci 1980;25:1587–99.
[6] Kim CY, Choi H-M, Cho HT. Effect of deacetylation on sorption of dyes and chromium on chitin. J Appl Polym Sci 1997;63:725–36.
[7] Hsien T-Y, Rorrer GL. Heterogeneous cross-linking of chitosan gel beads: kinetics, modeling, and influence on cadmium ion adsorption capacity. Ind Eng Chem Res 1997;36:3631.
[8] Aly AS, Jeon BD, Park YH. Preparation and evaluation of the chitin derivatives for wastewater treatments. J Appl Polym Sci 1997;65:1939–46.
[9] Zhou JL. Zn biosorption by *Rhizopus arrhizus* and other fungi. Appl Microbiol Biotechnol 1999;51:686–93.
[10] Furusawa T, Smith JM. Fluid-particle and intraparticle mass transport rates in slurries. Ind Eng Chem Fundam 1973;12:197–203.
[11] Fritz W, Merk W, Schlünder EU. Competitive adsorption of two dissolved organics onto activated carbon-II. Adsorption kinetics in batch reactors. Chem Eng Sci 1981;36:731–41.
[12] Findon A, McKay G, Blair HS. Transport studies for the sorption of copper ions by chitosan. J Environ Sci Health 1993;A28:173–85.
[13] Jansson-Charrier M, Guibal E, Roussy J, Delanghe B, Cloirec PL. Vanadium(VI) sorption by chitosan: kinetics and equilibrium. Water Res 1996;30:465–75.
[14] Weber WJ, Mathews AP. Effects of external mass transfer and intraparticle diffusion on adsorption rates in slurry reactors. In: American Institute of Chemical Engineers Symposium Series, vol. 73. New York, NY: American Institute of Chemical Engineers, 1962.
[15] Weber WJ, Morris JC. Advances in water pollution research: removal of biologically resistant pollutants from waste waters by adsorption. In: Proceedings of the International Conference on Water Pollution Symposium, vol. 2. Oxford: Pergamon Press, 1962.
[16] McKay G, Poots VJP. Kinetics and diffusion processes in colour removal from effluent using wood as an adsorbent. J Chem Tech Biotechnol 1980;30:279–92.
[17] McKay G, Blair HS, Findon A. Sorption of metal ions by chitosan. In: Eccles H, Hunt S, editors. Immobilisation of Ions by Biosorption. Chichester, UK: Ellis Horwood, 1986.

[18] Urano K, Tachikawa H. Process development for removal and recovery of phosphorus from wastewater by a new adsorbent-2. Adsorption rates and breakthrough curves. Ind Eng Chem Res 1991;30:1897–9.
[19] Hayward DO, Trapnell BMW. Chemisorption, second ed. London: Butterworths, 1964.
[20] Smith JM. Chemical Engineering Kinetics, third ed. New York, NY: McGraw-Hill, 1981.
[21] Bellot JC, Condoret JS. Modeling of liquid chromatography equilibrium. Process Biochem 1993;28:365–76.
[22] Yu J-W, Neretnieks I. Single-component and multicomponent adsorption equilibria on activated carbon of methylcyclohexane, toluene, and isobutyl methyl ketone. Ind Eng Chem Res 1990;29:220–31.
[23] Veglio F, Beolchini F. Removal of metals by biosorption: a review. Hydrometallurgy 1997;44:301–16.
[24] Sağ Y, Kaya A, Kutsal T. The simultaneous biosorption of Cu(II) and Zn on *Rhizopus arrhizus*: application of the adsorption models. Hydrometallurgy 1998;50:297–314.
[25] Snell FD, Snell CT. Colorimetric Methods of Analysis, third ed. New York, NY: Interscience, 1961.
[26] Van Vliet BM, Weber WJ Jr, Hozumi H. Modelling and prediction of specific compounds adsorption by activated carbon and synthetic adsorbents. Water Res 1980;14:1719–28.
[27] Mathews AP, Weber WJ Jr. Modeling and parameter evaluation for adsorption in slurry reactors. Chem Eng Commun 1984;25:157–71.
[28] McKay G, Bino MJ. Application of two resistance mass transfer model to adsorption systems. Chem Eng Res Dev 1985;63:168–74.
[29] Saucedo I, Guibal E, Roulph C, Le Cloirec P. Sorption of uranyl ions by a modified chitosan: kinetic and equilibrium studies. Environ Technol 1992;13:1101–15.
[30] Guibal E, Saucedo I, Roussy J, Roulph C, Le Cloirec P. Uranium sorption by glutamate glucan: a modified chitosan — Part II: Kinetic studies. Water SA 1993;19:119–26.
[31] Yang TC, Zall RR. Absorption of metals by natural polymers generated from seafood processing wastes. Ind Eng Chem Prod Res Dev 1984;23:168–72.
[32] Perry RH, Green D. Perry's Chemical Engineers' Handbook, sixth ed. New York, NY: McGraw-Hill, 1984.
[33] Tsezos M, Volesky B. The mechanism of uranium biosorption. Biotechnol Bioeng 1982;24:385–401.